Biophysical Journal, Volume *122*

Supplemental information

Location of dopamine in lipid bilayers and its relevance to neuromodulator function

Azam Shafieenezhad, Saheli Mitra, Stephen R. Wassall, Stephanie Tristram-Nagle, John F. Nagle, and Horia I. Petrache

Supplemental Materials

X-ray diffuse scattering

A background-subtracted x-ray diffuse scattering (XDS) image of an oriented and hydrated DLPC sample is shown in Fig. S1. Due to scattering noise, some of the pixel values become negative after background subtraction and those pixels are shown in red. The region of interest for data analysis is in the vicinity of scattering lobes on each side of specular reflection (detector meridian) at q_r = 527 pixels. The scattering on the meridian is due to the lamellar repeat and the peak centers can be used to calculate the lamellar repeat period, (D-spacing). For the diffuse part of the spectrum, an example of an analysis window is shown by the blue frame in Fig. S1. Also note that we have used multiple beamstops for different q_z ranges to account for higher overall scattering intensity at lower q_z. The blue box that includes the right sections of lobes 2 and 3 contains the data used to calculate the bending modulus K_C and the compression modulus B. As mentioned in Materials and Methods, besides the box that is shown in the figure, K_C and B were obtained using two additional fitting boxes with different lateral widths that are not shown.

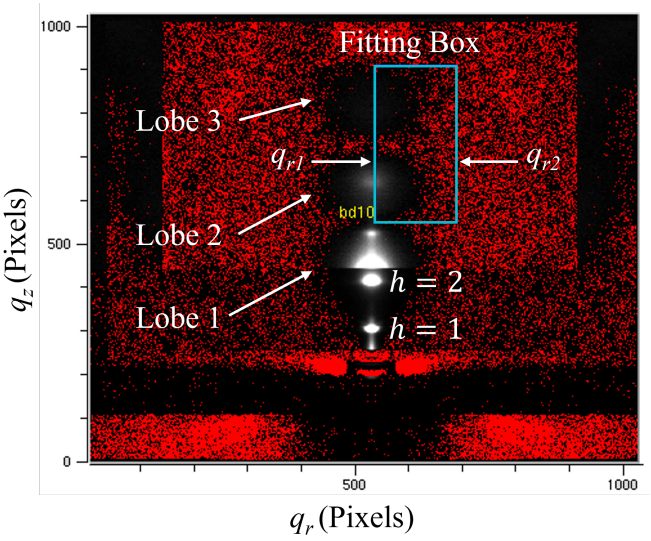

Figure S1: X-ray diffuse scattering of an oriented multilamellar DLPC sample at 25 °C showing an example of a fitting box used to calculate K_C and B. 100 pixels correspond to a q range of 1/nm. The h = 1 and h = 2 labels show the lamellar peaks used to calculate the D-spacing.

^{2}H Nuclear Magnetic Resonance

Representative ^{2}H NMR de-Paked spectra for POPC-d_{31}, POPS-d_{31}, and their mixtures with DA at 30 °C are shown in Fig. S2. A series of doublets that can be assigned to individual or groups of segments become resolved. The outer pair of peaks with greatest splitting are a composite of signals from ordered methylene groups in the upper part of the chain (C2-C10), while progressively less ordered methylene groups in the lower part (C10-C15) are responsible for the individual peaks with smaller splitting. The pair of peaks near the center at ± 2.5-3 kHz is due to the highly disordered terminal methyl groups (C16) at the bottom of the chain. The spectrum for POPS-d_{31} is wider than for POPC-d_{31}, which means that POPS is more ordered. Adding DA decreases the width of both POPC-d_{31} and POPS-d_{31} which implies lower order.

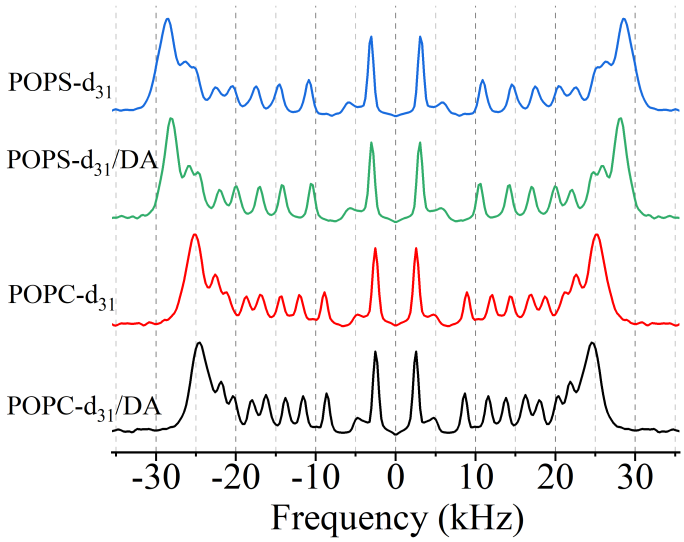

Figure S2: Representative ^{2}H NMR de-Paked spectra in the absence and presence of DA at 30 °C. The molar ratio of DA to lipid is 1:10.

Electron Paramagnetic Resonance

An example of an EPR spectrum of a 16-DSA paramagnetic probe in DOPC undergoing quasi-isotropic motion is shown in Fig. S3.

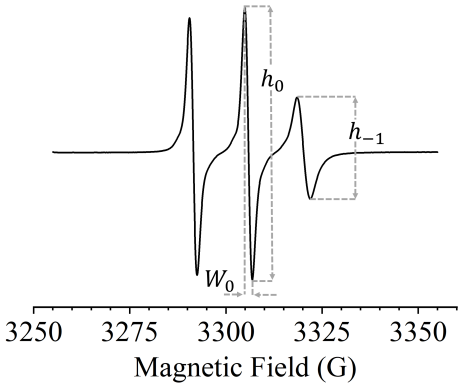

Figure S3: The EPR spectrum of a 16-DSA paramagnetic probe in DOPC at 25 °C. The ratio of lipid to 16-DSA was 100:1.

Fig. S4 shows the EPR spectra for 16-DSA and N-TEMPO probes incorporated into multilamellar vesicles of DOPC, DLPC, and DOPS lipids in the absence and the presence of DA. N-TEMPO measures changes near the lipid headgroup while 16-DSA measures changes near the bilayer center. Panel a shows the spectra of 16-DSA and panel b shows the spectra of N-TEMPO. Because of spectral width, the effect of DA is not easily visible in the figure. However, DA produces measurable differences in rotational correlation times τ_c that are calculated from the spectra.

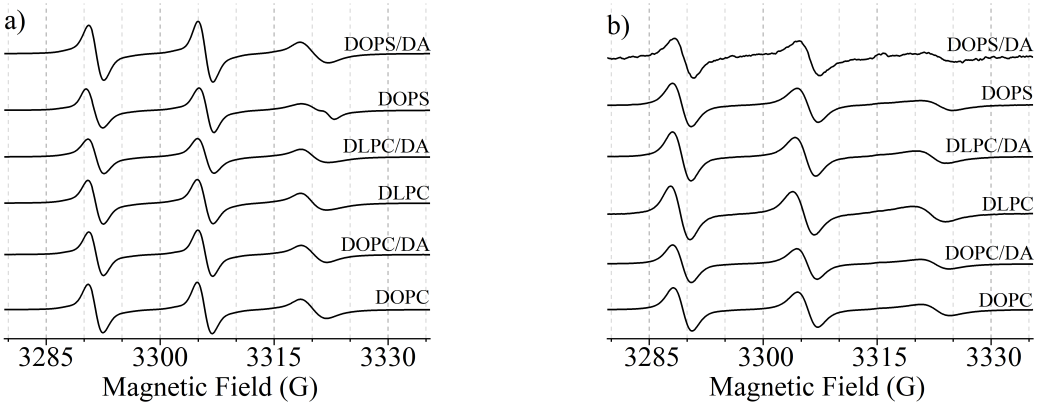

Figure S4: The EPR spectra of 16-DSA-labeled lipids and N-TEMPO-labeled lipids. for DOPC, DLPC, and DOPS in the absence and presence of DA at 25 °C. The molar ratio of DA to lipid and 16-DSA is 10:100:1 and the molar ratio of DA to lipid and N-TEMPO is 50:500:1. Panel (a) shows 16-DSA spectra and panel (b) shows N-TEMPO spectra.

Surface Plasmon Resonance (SPR)

Materials and Methods: SPR measurements were performed using an OpenSPR instrument (Nicoya, Kitchener, Ontario, CA). In these measurements, dopamine is considered to be the Ligand, and the solvent flowing over it is called the Analyte. Unless otherwise stated, the flow solvent was deionized water. DA was attached to the Sensor Chip using the following steps. Before starting, the chip was examined for bubbles, and the debubbling procedure was performed by flowing 80% isopropanol over the chip. The chip was cleaned with 10 mM HCl and rinsed with water. It was then activated by combining two reagents: 1-ethyl-3-(3-dimethyl aminopropyl) carbodiimide (EDC) and N-hydroxysuccinimide (NHS) (1:1, v:v) that were flowed over the chip. DA was immobilized by adding increasing concentrations, 10, 20 and 40 $\mu g/ml$ in NaAcetate buffer, pH 6.0, by first injecting, and then washing off excess DA. In each case, the Surface Plasmon Resonance response (SR) increased with the injection, then decreased slightly during the washing phase. After DA immobilization, the remainder of the activated sites on the chip were blocked with 1M ethanolamine, and then rinsed with DI water. At this point, unilamellar vesicles (ULVs) of DOPC or DLPC were added as the analyte. The injection phase was 300 seconds, and the wash phase was 900 seconds. The most successful measurements occurred at small lipid concentrations, 0.6 to 0.16 mg/ml. Higher concentrations caused artifacts, and smaller SRs. After measurements with ULVs were performed, a fresh chip was prepared in an identical way, except for the DA immobilization step. Unilamellar vesicles (ULVs) of DOPC and DLPC were flowed over the fresh chip, which served as the control.

Results: As shown in Figs. S5 and S6, ULVs of both DOPC and DLPC readily bound onto the DA-coated sensor chip. The control experiment also showed non-specific binding at the higher concentration of DOPC, and at both concentrations of DLPC ULVs. The control experiment was subtracted from the DA experiment in order to calculate $K_D = k_{\mathrm{off}}/k_{\mathrm{on}}$. The initial slope of binding or unbinding for all traces was determined using OriginPro.

For DLPC no unbinding was detected, but rather a continuing binding process after the wash phase, so K_D could not be determined for DLPC. This indicates that the binding of DLPC to DA is stronger than the binding of DOPC to DA. By contrast, when 150 mM PBS pH 7.0 was used as a control analyte there was rapid binding upon injection and rapid unbinding upon washing (data not shown), demonstrating that ULV binding is very different from control.

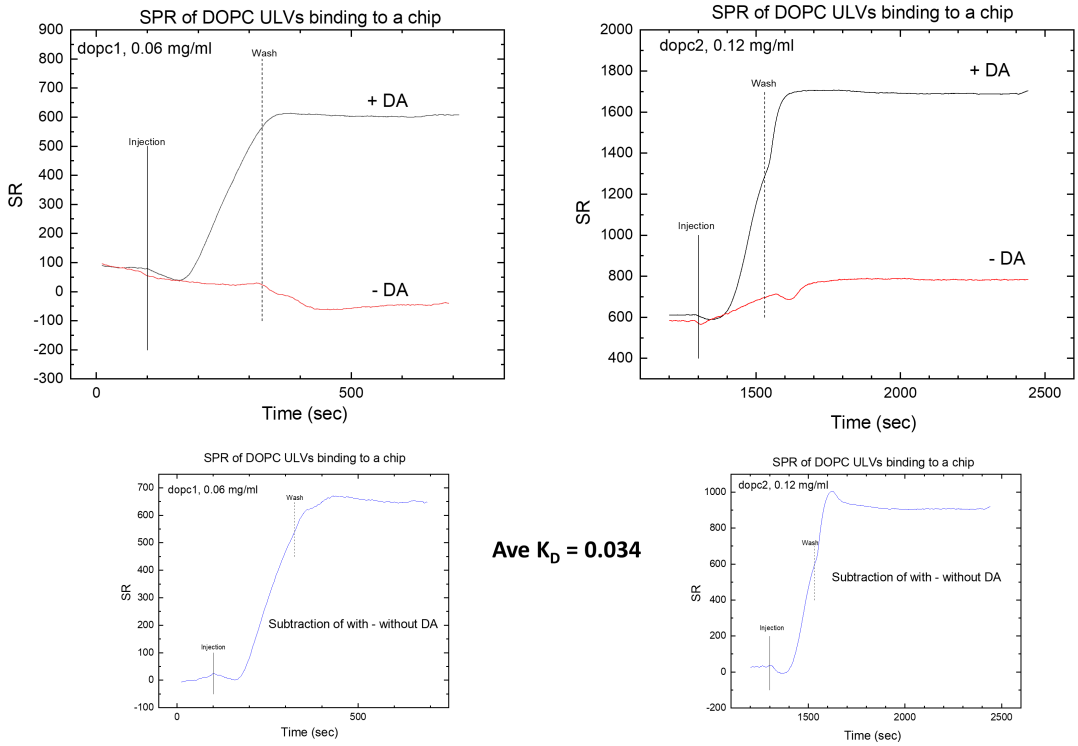

Figure S5: Surface Plasmon Resonance of DA association with DOPC membranes.

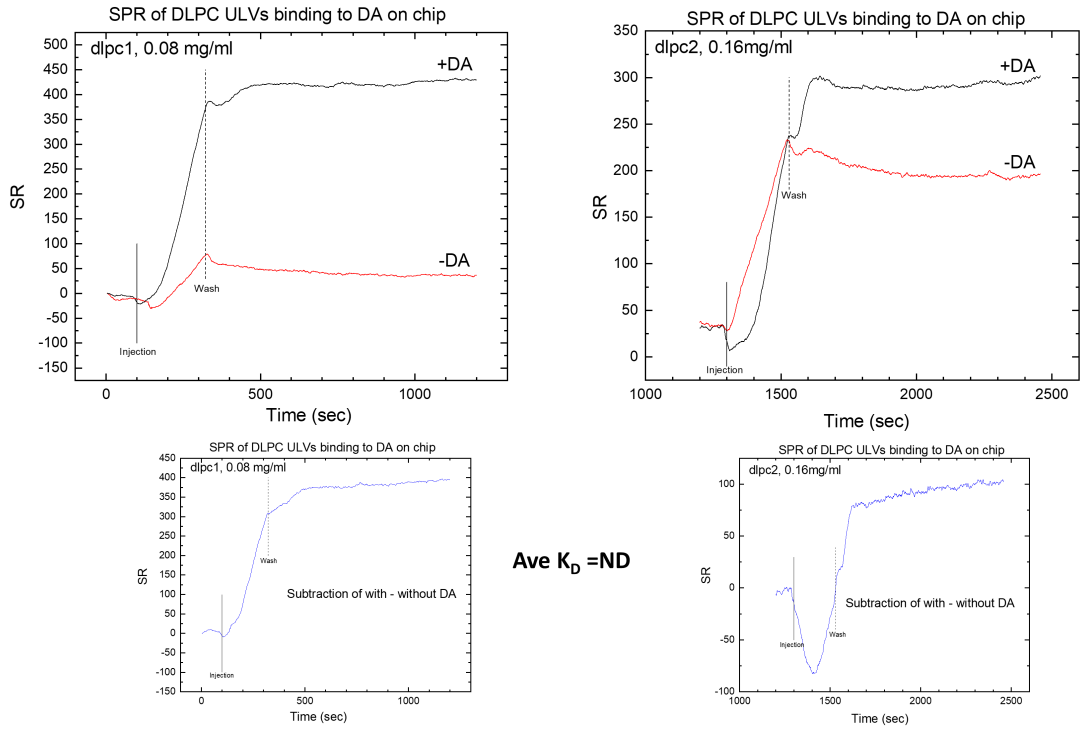

Figure S6: Surface Plasmon Resonance of DA association with DLPC membranes.

Acknowledgments

The authors would like to thank Dr. Berthony Deslouches in the Department of Environmental and Occupational Health of the Graduate School of Public Health at the University of Pittsburgh for the use of the SPR instrument. Support for this work was from National Science Foundation (NSF) MCB-2115790 (S.T.N., S.M.).